AGU PUBLICATIONS

JGR

Journal of Geophysical Research: Biogeosciences

RESEARCH ARTICLE

10.1002/2014JG002626

Key Points:
- Passive microwave indices can be used to estimate vegetation moisture
- Microwave observations were supported by flux data
- Passive microwave indices could be used to estimate evapotranspiration

Supporting Information:
- Text S1
- Text S2
- Figure S1
- Figure S2

Correspondence to:
V. Barraza,
vbarraza@iafe.uba.ar

Citation:
Barraza, V., F. Grings, P. Ferrazzoli, A. Huete, N. Restrepo-Coupe, J. Beringer, E. Van Gorsel, and H. Karszenbaum (2014), Behavior of multitemporal and multisensor passive microwave indices in Southern Hemisphere ecosystems, *J. Geophys. Res. Biogeosci.*, *119*, 2231–2244, doi:10.1002/2014JG002626.

Received 22 JAN 2014
Accepted 25 OCT 2014
Accepted article online 30 OCT 2014
Published online 18 DEC 2014

Behavior of multitemporal and multisensor passive microwave indices in Southern Hemisphere ecosystems

Veronica Barraza[1], Francisco Grings[1], Paolo Ferrazzoli[2], Alfredo Huete[3], Natalia Restrepo-Coupe[3], Jason Beringer[4], Eva Van Gorsel[5], and Haydee Karszenbaum[1]

[1]Institute of Astronomy and Space Physics (IAFE), CABA, Buenos Aires, Argentina, [2]DICII, Tor Vergata University, Rome, Italy, [3]Plant Functional Biology and Climate Change Cluster (C3), University of Technology, Sydney, New South Wales, Australia, [4]School of Earth and Environment, University of Western Australia, Crawley, Australia, [5]CSIRO Oceans and Atmosphere Flagship, Canberra, ACT, Australia

Abstract This study focused on the time series analysis of passive microwave and optical satellite data collected from six Southern Hemisphere ecosystems in Australia and Argentina. The selected ecosystems represent a wide range of land cover types, including deciduous open forest, temperate forest, tropical and semiarid savannas, and grasslands. We used two microwave indices, the frequency index (FI) and polarization index (PI), to assess the relative contributions of soil and vegetation properties (moisture and structure) to the observations. Optical-based satellite vegetation products from the Moderate Resolution Imaging Spectroradiometer were also included to aid in the analysis. We studied the X and Ka bands of the Advanced Microwave Scanning Radiometer-EOS and Wind Satellite, resulting in up to four observations per day (1:30, 6:00, 13:30, and 18:00 h). Both the seasonal and hourly variations of each of the indices were examined. Environmental drivers (precipitation and temperature) and eddy covariance measurements (gross ecosystem productivity and latent energy) were also analyzed. It was found that in moderately dense forests, FI was dependent on canopy properties (leaf area index and vegetation moisture). In tropical woody savannas, a significant regression (R^2) was found between FI and PI with precipitation ($R^2 > 0.5$) and soil moisture ($R^2 > 0.6$). In the areas of semiarid savanna and grassland ecosystems, FI variations found to be significantly related to soil moisture ($R^2 > 0.7$) and evapotranspiration ($R^2 > 0.5$), while PI varied with vegetation phenology. Significant differences ($p < 0.01$) were found among FI values calculated at the four local times.

1. Introduction

Numerous methodologies have been developed to estimate the different components of the surface hydrological balance (e.g., evapotranspiration (ET), soil moisture, and vegetation moisture) from remote sensing data. At regional scales, typical investigations have been based on the water balance equations, using satellite measurements in visible, near-infrared, and short-wave-infrared wavelengths as proxies [*Asrar et al.*, 1984; *Myneni et al.*, 1995; *Granger*, 2000; *Yebra et al.*, 2013]. These studies are based on the relation between reflectance (optical) and brightness temperature (near infrared) with leaf area index (LAI) and plant water content. However, these approaches present some limitations related to relatively low sensitivity to vegetation moisture and low temporal resolution (mostly due to cloud cover and atmospheric effects). To overcome some of these limitations, a new technique that links vegetation properties and latent energy (LE) fluxes to microwave data was proposed by *Min and Lin* [2006] and *Li et al.* [2009]. Although characterized by coarser spatial resolutions, passive microwave sensors can be useful for long-term and large-scale applications, since they offer shorter revisit times and are less affected by atmospheric conditions compared to optical systems.

Microwave indices are known to be mainly sensitive to (i) vegetation moisture [*Ferrazzoli et al.*, 1992; *Min and Lin*, 2006; *Barraza et al.*, 2014] and (ii) soil moisture [*Jackson*, 1997]. Therefore, microwave indices are theoretically related to surface mass/energy balance and to ET. Although the key processes which relate ET to microwave indices will be the same (the sensitivity to vegetation and soil moisture), this relation will depend on the key geometrical and dielectric characteristics of the land cover. Following this hypothesis, in the current work, the differences in the relation between ET and passive microwave indices sensitive to different

land surface parameters across different ecosystems were evaluated. Numerous studies have been undertaken to relate microwave indices with ET and canopy CO_2 exchange [*Min and Lin*, 2006; *Li et al*., 2009; *Jones et al*., 2012], but there are few studies involving multiyear [*Jones et al*., 2012] and multisensor data sets [*Li et al*., 2009] and no direct applications of such data sets across different ecosystems.

Among these studies, interestingly, *Li et al*. [2009] shows that hourly observations (derived from different orbital platforms) can provide the opportunity to repetitively measure high-frequency variations of passive microwave signals, which can be related to diurnal changes in vegetation and soil properties. In principle, during a single day, there are five factors that can produce changes in microwave brightness temperature observations: (1) changes in soil and vegetation temperature, (2) changes in soil moisture, (3) changes in vegetation moisture, (4) acquisition during a rain event, and (5) presence of free water over the vegetation. On the other hand, at seasonal temporal scales, there are primarily four factors that can produce changes in brightness temperature observations: (6) changes in vegetation structure and biomass (e.g., leaf area index (LAI)), (7) seasonal changes in soil or vegetation temperature, (8) seasonal changes in soil moisture, and (9) seasonal changes in vegetation moisture. If we want to use microwave data to monitor soil and vegetation moisture at hourly and seasonal scale (2, 3, 8, and 9), we first need to analyze and discard the contribution of the other possible effects described above.

Normalized indices such as microwave emissivity difference vegetation index (EDVI), polarization index (PI), and frequency index (FI) are, in most cases, independent of thermodynamic temperature (1 and 7). However, over some areas such as sand dunes, small brightness temperature diurnal cycles have been observed, which are not consistent with the diurnal variations of skin temperature [*Prigent et al*., 1999; *Norouzi et al*., 2012]. These studies show that in sandy soils, the observed microwave emission comes from deeper layers rather than from the surface skin and the observed signal depends on the frequency and soil temperature profile [*Prigent et al*., 1999]. It is also relevant to mention that the emission is strongly affected by the presence of rainfall during an acquisition due to the important contribution of cold raindrops to the overall emissivity (4 and 5). In all other cases (no sandy soil and no rain), the emissivity should primarily depend on vegetation and soil moisture. Vegetation attenuation of soil emission depends on the vegetation moisture content, biomass, and structure, as well as instrument wavelength [*Engman and Chauhan*, 1995]. Consequently, in general, the vegetation canopy becomes more transparent at longer wavelengths.

For areas where vegetation biomass is moderate or high, the canopy contribution is dominant (particularly at X band and higher frequencies). Therefore, in the above-mentioned cases, microwave frequency indices (FI or EDVI) should become a function of canopy properties, i.e., structure of leaves and stems and moisture content [see, e.g., *Paloscia and Pampaloni*, 1992; *Ferrazzoli et al*., 1995]. Since canopy structure exhibits relatively slow temporal variations relative to changes in canopy moisture, microwave frequency indices will show a slow seasonal component associated with subtle changes of canopy properties and a higher-frequency component associated with canopy moisture variations.

Over a single day, the vegetation properties that control the overall microwave emissivity are expected to remain constant, with the exception of vegetation moisture. Therefore, an hour-to-hour analysis of microwave indices is particularly interesting, since it should be mainly related to changes in vegetation moisture (i.e., plant water stress due to environmental factors [*Li et al*., 2009]). In this framework, it is interesting and promising to investigate the potential of microwave indices derived from different platforms to obtain information on vegetation and soil moisture for contrasting ecosystem types. When biomass is low or moderate, soil emission also plays an important role, and the overall signal will become a function of soil and vegetation moisture.

Although vegetation and soil moisture are just two components of the overall water balance, they are important variables in the surface radiation and water budgets, which effectively modulate ET, even though the relation may be very complex and land cover dependent. Therefore, the main objective of this study is to assess the relative contributions of soil and vegetation properties to variations in microwave indices using multitemporal and multisensor observations for potential ET retrieval applications. In particular, in this manuscript, we have addressed the following questions: What are the daily and seasonal patterns of microwave indices in the study area? What are the relative contributions of the soil and vegetation canopy to microwave indices? And finally, are passive microwave indices good proxies for ET for different ecosystems? To this aim, we analyzed hourly and seasonal time series of passive microwave data along with optical

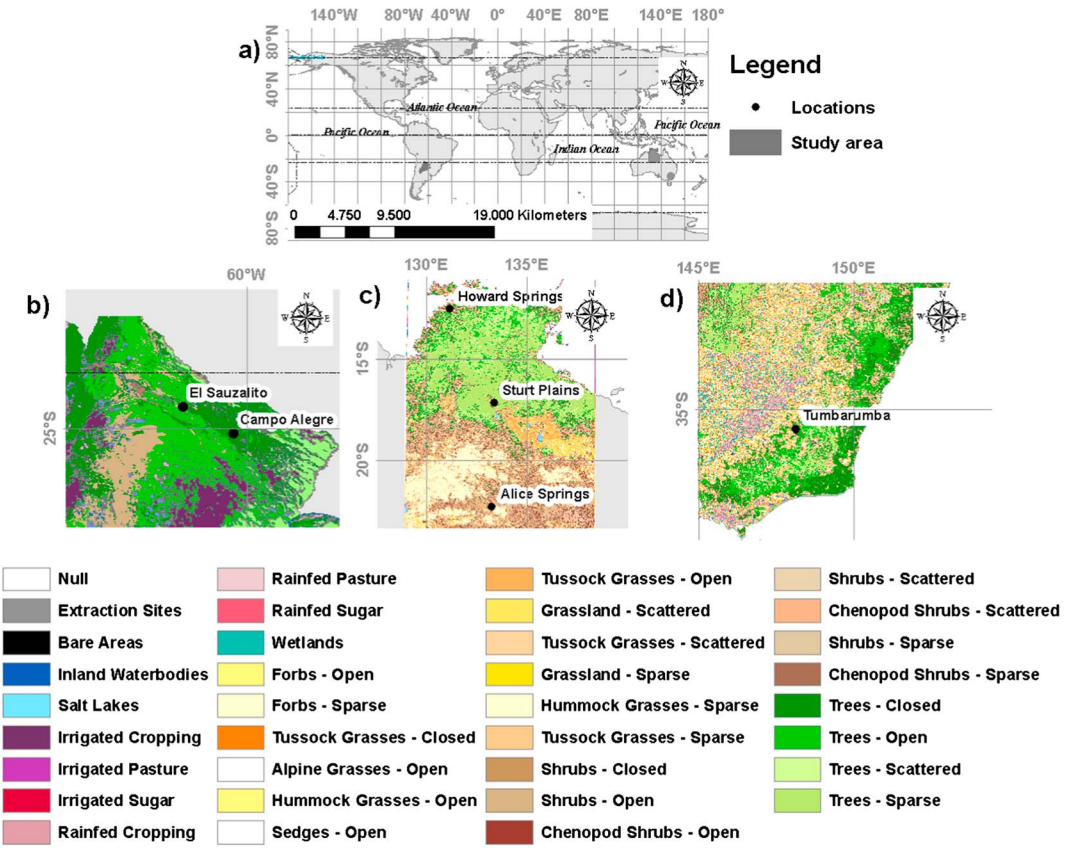

Figure 1. (a) Land cover map of the study areas located in (b) Argentina and in (c and d) Australia.

vegetation indices, meteorological data, and flux tower data for six different tropical and subtropical ecosystems in the north and southwest of Australia and northwest Argentina. Finally, eddy covariance flux data were used to evaluate the relationship between microwave indices and latent energy (LE).

2. Materials

2.1. Study Areas

We focused our investigation over natural vegetation areas located in the Southern Hemisphere over two continents, north and southeast of Australia and northwest of Argentina (Figure 1). The study areas were selected as they offer an array of ecosystems where we can test the potential of microwave indices for monitoring different vegetation and soil properties (moisture and structure). The selected areas are characterized by the occurrence of a predictable wet and dry season [*Taylor and Tulloch*, 1985; *González and Flores*, 2010]. Moreover, all the study areas are large homogeneous regions, which made it possible the use of passive microwave signatures characterized by low spatial resolution. According to the International Geosphere-Biosphere Programme data [*Hansen and Reed*, 2000] and the national classification scheme [*Morello*, 1974], these sites are located across a wide range of land cover types including deciduous open forest, tropical woody and semiarid savannas, and grasslands (Table 1). The sites span a large wet-to-dry gradient starting with the wettest site being in the Australian tropical north, Howard Springs, which is characterized by 2000 mm/yr mean annual precipitation [*Hutley et al*., 2011; *Kanniah et al*., 2011]. Rainfall decreases toward the continental interior of Australia, reaching ~100 mm/yr in Alice Springs, in the center of the continent [*Cleverly et al*., 2013; *Eamus et al*., 2013]. Rainfall over the northern Australia is highly seasonal, with a wet season during the summer and extending December to March, and dry cycle during April to October that includes the coldest months. These sites are located across vast undulating sandy to sandy clay loam plains interspersed with cracking clay plains [*Hutley et al*., 2011]. We also included one site in the

Journal of Geophysical Research: Biogeosciences 10.1002/2014JG002626

Table 1. Summary of Available Ground Data[a]

Name	Location	Elev (m)	Veg. Height (m)	LAI	DBH (cm)	Biomass (t/ha)	Stem den. (1/ha)	Surface Soil Texture Represented by the Tower Sites	Average Surface Soil Texture	Biome	Land Cover	Prec. (mm/yr)
Howard Springs	12.8°S, 131.3°E	64	15–18[f]	1.04 ± 0.07[d]	8.8–30.4[b]	62.4[c]	661[c]	Red kandosol with ironstone gravels[b]	Sandy loams	Tropical rainforest	Open woodland savanna	1750[f]
Alice Springs	22.3°S, 133.2°E	606	6.5[e]	Overstory 0.18–0.3, understory 0.04–0.32[d]	11[b]	Not applicable (NA)	820[e]	Red kandosol	Sandy loams	Semiarid desertand xeric shrublands	Semiarid savanna (mulga)	305.9[f]
Sturt Plains	17.2°S, 133.4°E	210	0.1[f], 0.2[c]	0.39[c]	-	NA	-	Black cracking clays[b]	Sandy loams/ clay loams	Grass savanna	Low grassland plain	640[f], 535[c]
Tumbarumba	35.7°S, 148.2°E	1200	40	2.47	22 ± 1.7[g]	NA	850 ± 170	-	Sandy loams/ clay loams	Wettemperate sclerophyll eucalypt	Cold temperate forest	1000
El Sauzalito	61.68°S, 24.417°W	140	20–25	1–3	10–30[h]	70–1l10[h]	133[h]	-	Silt loam	Dry Chaco Forest	Xerophytes forest	500
Campo Alegre	60.18°S, 25.8°W	138	20–25	2.5	10–30[h]	70–110[h]	130[h]	-	Silt loam	Dry Chaco Forest	Xerophytes forest	700

[a]LAI is leaf area index, Elev is elevation taken above sea level, DBH is the diameter at 1.3 m height, Veg. Height is vegetation height, Stem den. is stem density, Biomass is ecosystem biomass, and Prec. is precipitation. Mean annual rainfall is from 1998 to 2012 from Tropical Rainfall Measuring Mission (TRMM) [*NASA*, 2013] data [*NASA*, 2014b]. Tropical Rainfall Measuring Mission Project (TRMM), 3B43: monthly 0.25 × 0.25° merged TRMM and other estimates v7. NASA Distribution. Active Arch. Cent., Goddard Space Flight Cent. Earth Sci., Greenbelt, Md. URL http://mirador.gsfc.nasa.gov/cgi-bin/mirador/ (accessed 2.27.14). Average surface soil texture at 25 × 25 km of spatial resolution from the Atlas of Australian Soils and Atlas de Suelos de la República Argentina Instituto de Suelos–INTA.
[b]*Eamus et al.* [2000].
[c]*Hutley et al.* [2011].
[d]*Sea et al.* [2011].
[e]*Eamus et al.* [2013].
[f]Information available at http://www.ozflux.org.au.
[g]*Leuning et al.* [2005].
[h]*Gasparri and Baldi* [2013].

Table 2. Spectral Indices Calculated From AMSR-E, WindSat, and MODIS Including Their Acronym, Mathematical Formulation, and References[a]

Index	Formulation	Reference
Frequency index	$FI = \frac{Tbv\ (Ka\ band) - Tbv\ (X\ \ band)}{Tbv\ (Ka\ band) + Tbv\ (X\ \ band)} * 2$	*Ferrazzoli et al.* [1995]
Polarization index	$PI = \frac{Tbv\ (X\ \ band) - Tbh(X\ \ band)}{Tbv\ (X\ \ band) + Tbh(X\ \ band)} * 2$	*Paloscia and Pampaloni* [1988]
Enhanced vegetation index	$EVI = \frac{2.5\ *\ 2(1)}{(2+6\ *\ 1+6.5\ *\ 3+1)}$	*Huete et al.* [2002]

[a]Parameter ρx is the reflectance in MODIS X band (1 to 3), T_b is the brightness temperature, and *v* and *h* suffixes indicate vertical and horizontal polarization, respectively.

southeast of Australia (Tumbarumba) with high biomass [*van Gorsel et al.*, 2013; *Leuning et al.*, 2005] to make comparisons with an Argentinean site (Dry Chaco Forest, which is a dry forest phytogeographic region). Rainfall occurs predominantly during the winter months at Tumbarumba (June to August). In the northwest of Argentina, across an east to longitudinal transect (Figure 1), the annual rainfall decrease from east (1400 mm) to west (300 mm). Campo Alegre is located at the center of this gradient at about 700 mm mean annual precipitation and El Sauzalito at the western end with ~500 mm rainfall. These last two areas are located in the Dry Chaco Forest, which is mainly an open dry forest characterized by austral summer rainfall.

2.2. Data Sets

We processed microwave data collected by the Advanced Microwave Scanning Radiometer–EOS (AMSR-E/Aqua) [*Kawanishi et al.*, 2003] and Wind Satellite (WindSat/Coriolis) [*Gaiser et al.*, 2004] in both ascending and descending overpasses from 2007 to 2009, in order to closely examine the diurnal behavior of the microwave signals. Four observations were collected per day, at four different local solar times: AMSR-E descending: 1:30 h, WindSat descending: 6:00 h, AMSR-E ascending: 13:30 h, and WindSat ascending: 18:00 h. Furthermore, we included data from the Moderate Resolution Imaging Spectroradiometer (MODIS) land surface reflectance product at 500 m spatial resolution (MYD09A1) [*Vermote and Vermeulen*, 1999] and MODIS leaf area index (LAI) product (MYD15A2) [*Myneni et al.*, 1997] in the analysis. AMSR-E and MODIS data were downloaded from the National Aeronautics and Space Administration (NASA) data depository (http://reverb.echo.nasa.gov/). WindSat data were provided by the United States Naval Research Laboratory.

2.3. Microwave and Optical Indices

Taking advantage of the high temporal resolution of microwave systems, we evaluated the seasonal and hourly patterns of the polarization index (PI) [*Paloscia and Pampaloni*, 1988] and the frequency index (FI) [*Ferrazzoli et al.*, 1995], calculated using the brightness temperatures measured at 37 GHz (Ka band) and 10.6 GHz (X band) for both AMSR-E and WindSat (equation at Table 2). We used FI calculated at vertical polarization since it showed a higher correlation with vegetation state properties [*Min and Lin*, 2006]. In this study, observations during precipitation events were excluded from the analysis with the aid of in situ precipitation data. The diurnal variations of the signals derived from WindSat and AMSR-E should be related to changes on surface characteristics, as both sensors are intercalibrated [*Das et al.*, 2014] and have similar characteristics, including central frequency and bandwidth for all bands, an incidence angle of 55°, and a conical scanning technique.

PI and FI are complex aggregate functions of vegetation (biomass, LAI, geometric structure, and moisture content) and soil (roughness and moisture content) surface conditions [see *Ferrazzoli et al.*, 1992; *Paloscia and Pampaloni*, 1992; *Ferrazzoli et al.*, 1995]. In order to evaluate the contribution of the vegetation canopy to passive microwave indices, we compared the 8 day PI and FI values with the enhanced vegetation index (EVI), computed using the MODIS 8 day composited reflectance product (Table 2). Lower quality data and data with partial or complete cloud cover were removed from the analysis using the quality assessment information.

2.4. Environmental Drivers and Eddy Covariance Flux Measurements

In order to evaluate the sensitivity of microwave indices to environmental variables, we analyzed a time series of data from flux towers located in three Australian study sites with data available from 2007 to 2009 (Howard Springs [*Beringer*, 2013a], Sturt Plains [*Beringer*, 2013b], and Tumbarumba [*van Gorsel*, 2013]). The original data

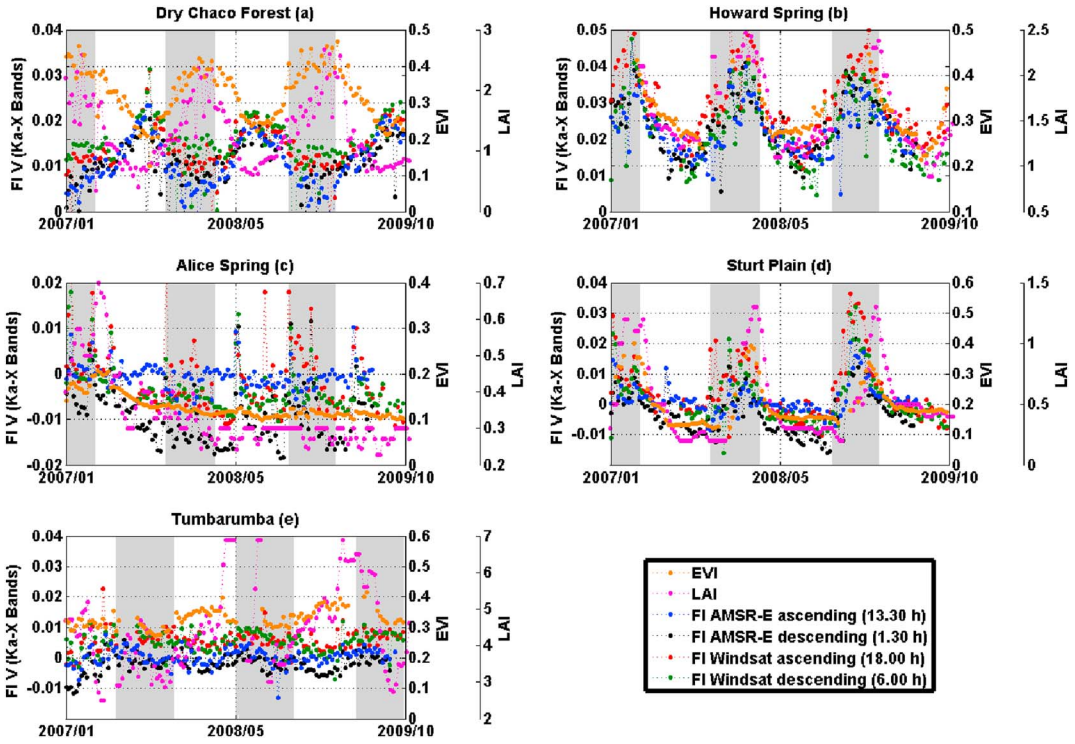

Figure 2. Eight-day FI, EVI, and LAI time series data for 2007–2009. The selected sites correspond to (a) open forest (Dry Chaco Forest), (b) tropical open woodland savanna (Howard Springs), (c) semiarid savanna (Alice Springs), (d) grassland (Sturt Plains), and (e) wet temperate sclerophyll eucalypt forest (Tumbarumba).The shaded area corresponds to the period December to March (wet season) for Figures 2a to 2d and May to August (wet season) for Figure 2e.

were provided by the OzFlux network (http://ozflux.its.monash.edu/ecosystem/home.jspx) and preprocessed to ensure consistency among sites; this included general removal of outliers and faulty data and removal of low turbulence periods. Eddy covariance data sets were quality assured and quality controlled (QC) using the OzFlux standard processing protocol OzFluxQC v2.7.1, which was developed under creative common licensing by the OzFlux community using Python (Enthought Python Distribution version 7.3-1), the process involves making a range test and removal of data spikes, removal of fluxes where more than 1% of 10 Hz observations are missing from the 30 min average, linear corrections for sensor drift and calibration changes, and rejection of observations when wind originated from behind the 3-D anemometer and tower.

Hourly averages of latent energy flux (LE (W/m^2)) and surface temperature at −8 cm depth (°C) were analyzed. LE is related to evapotranspiration as ET = LE/lambda, where lambda is the latent heat of vaporization. Hourly fluxes of gross ecosystem productivity (GEP) were derived as GEP = NEE-Reco, where NEE is net ecosystem exchange measured at the tower and Reco is the ecosystem respiration. A second-order Fourier regression was fitted to the nighttime NEE series, which is assumed to be representative of Reco, using the method proposed by *Richardson and Hollinger* [2005]. For seasonal analysis, we aggregated hourly fluxes and other meteorological data to daily values, where at least 21/24 h of observations were available and later to an 8 day time periods if at least 2/8 days were available.

In addition to the flux and meteorological measurements (precipitation), we used satellite-derived data from the Tropical Rainfall Measuring Mission (TRMM, product 3B42, v7, *NASA*, 2010) to obtain a consistently filled precipitation time series across all sites. Although noisy, the use of TRMM data is justified by the observed correlation between TRMM and available tower data. For the Sturt Plains and Howard Spring sites, observations of volumetric soil moisture (%/%) at −8 cm depth were available, as measured by a water content reflectometer (CS616). Micrometeorological variables were available at seasonal and hourly scales (0:00–2:00 h, 5:00–7:00 h, 12:00–14:00 h, and 17:00–19:00 h). A linear regression (type II) analysis was made between microwave indices and environmental drivers and eddy covariance flux measurements. A linear correlation analysis was made between both microwave indices.

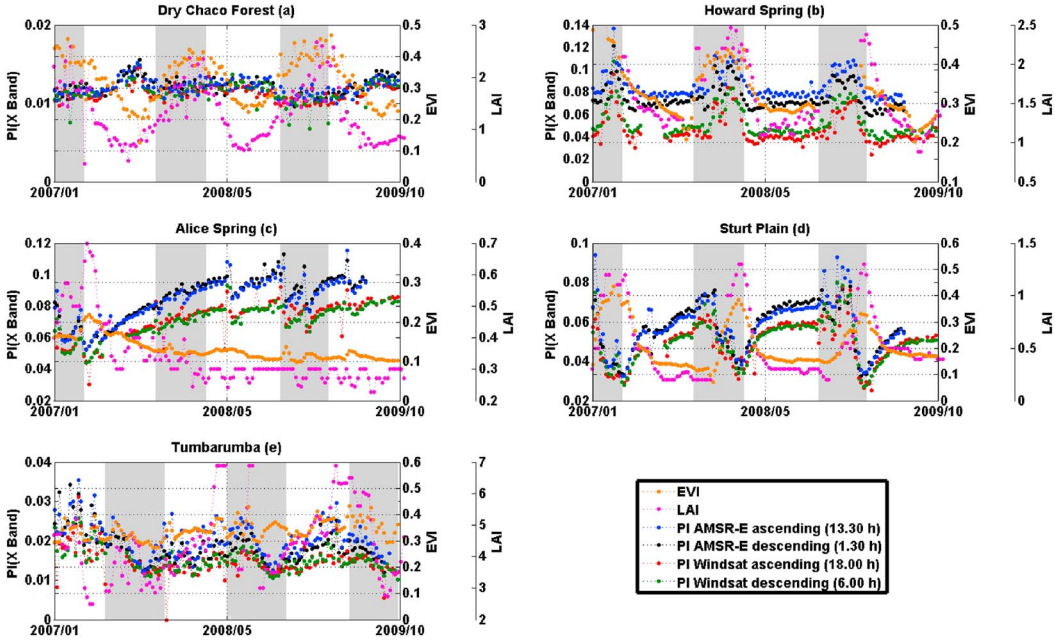

Figure 3. Eight-day PI, EVI, and LAI time series data for 2007–2009. The selected sites correspond to (a) open forest (Dry Chaco Forest), (b) tropical open woodland savanna (Howard Springs), (c) semiarid savanna (Alice Springs), (d) grassland (Sturt Plains), and (e) wet temperate sclerophyll eucalypt forest (Tumbarumba). The shaded area corresponds to the period December to March (wet season) for Figures 3a to 3d and May to August (wet season) for Figure 3e.

3. Results

3.1. Seasonal Patterns of Passive Microwave Indices

We observed different seasonal behaviors of the microwave indices in the analyzed study areas (Figure 2a). Data from El Sauzalito and Campo Alegre in the Dry Chaco Forest showed very similar trends of LAI, EVI, FI, and PI for all acquisitions in the time frame analyzed (Figures 2a and 3a). For this reason, the data collected in these two sites was aggregated (average) and shown in unique plots, collectively labeled as "Dry Chaco Forest." For the Dry Chaco Forest (Figures 2a and 3a), PI values were low, and FI values were inversely and

Table 3. Summary of Determination Coefficients (R^2) for the Time Series MODIS, AMSR-E, and WindSat[a]

Name	Land Cover		FIAA	FIAD	FIWA	FIWD	PIAA	PIAD	PIWA	PIWD
Howard Springs	Open woodland savanna	EVI	0.37[c]	0.45[c]	0.54[c]	0.40[c]	0.35[c]	0.28[b]	0.31[c]	0.35[c]
		LAI	0.51[c]	0.65[c]	0.64[c]	0.65[c]	0.51[c]	0.32[c]	0.39[c]	0.52[c]
		GEP	0.47[c]	0.69[c]	0.59[c]	0.41[c]	0.61[c]	0.50[c]	0.45[c]	0.48[c]
Alice Springs	Semiarid savanna	EVI	0.10	0.21[b]	0.13	0.28[b]	0.62[c]	0.72[c]	0.69[c]	0.68[c]
		LAI	0.03	0.07	0.04	0.11	0.57[c]	0.56[c]	0.65[c]	0.68[c]
		GEP	-	-	-	-	-	-	-	-
Sturt Plains	Low grassland plain	EVI	0.14	0.27	0.15	0.24	0.34[c]	0.59[c]	0.49[c]	0.36[c]
		LAI	0.15	0.30[b]	0.16	0.25[b]	0.33[b]	0.58[c]	0.45[c]	0.33[c]
		GEP	0.31[c]	0.39[c]	0.52[c]	0.55[c]	0.26[b]	0.58[c]	0.45[c]	0.33[b]
Tumbarumba	Cold temperate forest	EVI	NS[d]	NS[d]	NS[d]	NS[d]	0.04	NS[d]	0.03	0.01
		LAI	NS[d]	NS[d]	NS[d]	NS[d]	0.12	0.07	0.08	0.10
		GEP	0.10	NS[d]	NS[d]	NS[d]	NS[d]	NS[d]	NS[d]	0.10
Chaco Forest	Xerophytes forest	EVI	0.54[c]	0.33[c]	0.29[b]	0.10	0.12[b]	0.12[b]	0.10	0.14[b]
		LAI	0.67[c]	0.24[b]	0.34[c]	0.17[b]	0.20[b]	0.25[b]	0.20[b]	0.30[c]
		GEP	-	-	-	-	-	-	-	-

[a]PI stands for polarization index; FI for frequency index; and AA, AD, WA, and WD for AMSR-E ascending, AMSR-E descending, WindSat ascending, and WindSat descending. LAI is the leaf area index, and GEP is the gross ecosystem productivity.
[b]Significant regression at $\alpha = 0.01$.
[c]Significant regression at $\alpha = 0.001$.
[d]NS is not significant.

Table 4. Summary of Determination Coefficients (R^2) for the Time Series AMSR-E and WindSat, Soil Moisture (SM), and Precipitation (Prec)[a]

Name	Land Cover		FIAA	FIAD	FIWA	FIWD	PIAA	PIAD	PIWA	PIWD
Howard Springs	Open woodland savanna	Prec	0.22[b]	0.41[c]	0.56[c]	0.38[c]	0.50[c]	0.52[c]	0.52[c]	0.51[c]
		SM	0.61[c]	0.67[c]	0.64[c]	0.71[c]	0.77[c]	0.55[c]	0.74[c]	0.64[c]
Alice Springs	Semiarid savanna	Prec	NS	0.13	0.17[b]	0.14	NS	NS	NS	NS
Sturt Plains	Low grassland plain	Prec	0.20[b]	0.28[b]	0.54[c]	0.37[c]	0.21[b]	NS	0.10	0.22[b]
		SM	0.74[c]	0.77[c]	0.82[c]	0.87[c]	0.46[c]	NS	0.64[c]	0.22[b]

[a]PI stands for polarization index; FI for frequency index; and AA, AD, WA, and WD for AMSR-E ascending, AMSR-E descending, WindSat ascending, and WindSat descending.
[b]Significant regression at $\alpha = 0.01$.
[c]Significant regression at $\alpha = 0.001$.
[d]NS is not significant.

significant related to MODIS EVI and MODIS LAI (Figures 2a and 3a and Table 3). The seasonal behavior of FI showed a decrease in austral summer and an increase in austral winter, opposite to MODIS EVI and LAI.

At Howard Springs, the long-term temporal trend was different from the Dry Chaco Forest (Figures 2b and 3b). Here the trends of both FI and PI were positively significant related to MODIS EVI and LAI (Table 3) with higher values of FI corresponding to EVI > 0.3. There was also a positive and significant relation between the passive microwave indices and gross ecosystem productivity (GEP) calculated from flux tower data (Table 3). At the Howard Springs tropical woody savanna site, the EVI seasonal signal responded to and was synchronous with the arrival of the monsoonal rains during the spring-summer transition [*Ma et al.*, 2013]. Since higher FI and PI values were present during the rainy season (austral summer precipitation) and the biomass of this site was moderate, a consistent explanation of the observed FI and PI trends could be related to a significant contribution of soil to overall emissivity. In fact, we found a strong and significant relation between FI, PI, and 8 day precipitation and soil moisture (see Table 4).

The time series of FI, PI, EVI, and LAI for Alice Springs and Sturt Plains are shown in Figures 2c and 2d and Figures 3c and 3d. The LAI of these areas was lower (LAI < 1), and the climate was much drier than at Howard Springs. FI of both sites showed a moderate positive relation with EVI. Interestingly, PI values of both sites showed an inverse trend with MODIS EVI and LAI, resulting in significant and negative relation with EVI and LAI (Table 3). At Alice Springs, this could be due to a prolonged vegetation drying phase from 2007 to 2008 as reported by *Ma et al.* [2013] (Figure 4). By contrast, at Sturt Plains, the temporal trend of PI was more complex. At this site, rainfall initially produced an increase in PI but was followed by decreases in PI inversely related to EVI and LAI (since rainfall initiated the subsequent vegetation growth) (Figures 3 and 4). This was further followed by a long dry spell interval during which vegetation became dry and PI increased again.

As higher FI and PI values were encountered during the rainy season (Figure 4), in agreement with theoretical relationships involving soil moisture, we also evaluated the relation between FI and precipitation. Overall, the results (Table 4) showed a significant relation between precipitation and FI at Sturt Plains (Table 4). In addition to this, we evaluated the seasonal relationship between soil moisture (m^3/m^3) and microwave indices for the Sturt Plains site, where in situ soil moisture data were available. We found a significant relation between soil moisture and FI and between soil moisture and PI for the observations before 6:00 h at the grassland site.

Finally, at the Tumbarumba site, the FI and PI time series (Figures 2e and 3e) did not show a strong seasonal variation, since the forest is relatively dense and evergreen. As shown in Figures 2e and 3e and Table 3, there was a nonsignificant relation between EVI and the microwave indices, while PI showed a nonsignificant relation with LAI. We analyzed the relationship between PI and GEP calculated from flux tower data (Table 3). We found a nonsignificant determination coefficient between PI and GEP (Table 3). The magnitude of both passive microwave indices was low and within the same range of values as encountered at the Dry Chaco Forest site.

3.2. Hourly Behavior Across the 8 Day of Passive Microwave Time Series

For Chaco Forest, the FI values obtained by WindSat (6:00 h and 18:00 h) were, on average, the highest observed (Figure 2a). It was observed that the hourly behavior changed according to different seasons. Significant differences (analysis of variance (ANOVA), $F = 211.57$, $p < 0.01$, $n = 136$) were found between FI

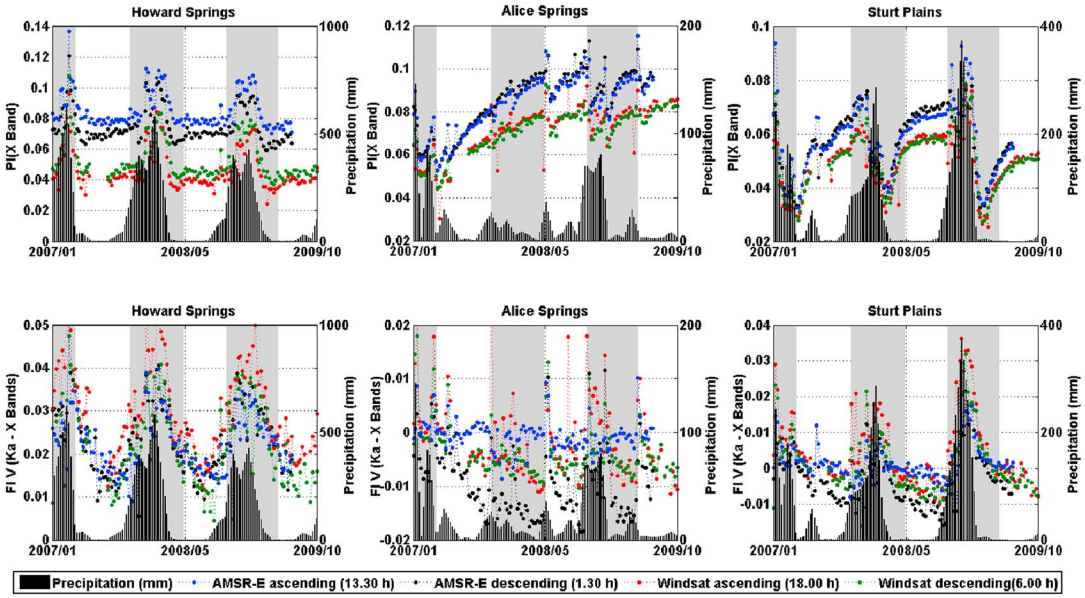

Figure 4. Eight-day PI, FI, and precipitation (mm) time series data for 2007–2009. The shaded area corresponds to the period December to March (wet season).

from austral summer (December–February) versus winter (June–August). In particular, the hourly spread of FI observations was large during austral summer and low or negligible during austral winter. In summer, the mean FI at Dry Chaco Forest (Figure 5) increased from 0.008 to 0.013 for observations acquired during the 1:30 h–18:00 h period, then strongly decreased to 0.006 during the 13:30 h overpass, and finally increased back to 0.015 again at 18:00 h. It is worthwhile to note that these variations (1) are only present in summer and (2) are larger than the expected radiometric error in FI (maximum error ~0.0025, assuming uncorrelated radiometric errors ~1 K for both bands (V and H)). Significant differences (ANOVA, $F = 54.57$, $p < 0.01$, $n = 35$) were found among FI values calculated at the four local times during summer.

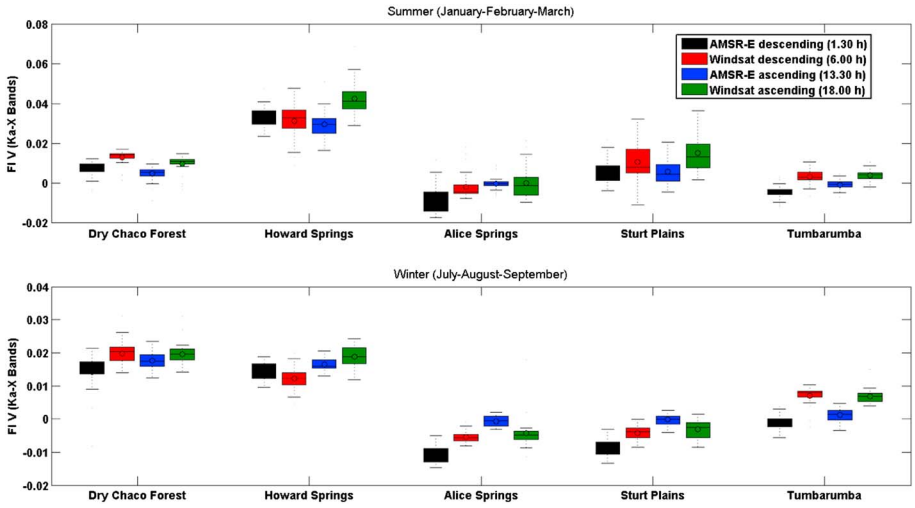

Figure 5. Boxplots of summer and winter 8 day FI time series for 2007–2009. The whiskers extend out to the maximum or minimum value of the data for each season, (top) summer and (bottom) winter.

Table 5. Summary of Determination Coefficients (R^2) Between the Hourly Time Series of Surface (T_s) With Hourly FI Observations Calculated From AMSR-E and WindSat Time Series

Name	Land Cover	Jan	Feb	Mar	Apr	May	Jun	Jul	Aug	Sep	Oct	Nov	Dec
Howard Springs	Open woodland savanna	0.42[b]	0.43[b]	0.27[a]	0.11	0.63[b]	0.64[b]	0.88[b]	0.92[b]	0.56[b]	0.29[b]	NS[c]	0 NS[c]
Sturt Plains	Low grassland plain	0.22[a]	0.29[a]	-	-	0.69[b]	0.74[b]	0.41[b]	0.63[b]	0.63[b]	0.74[b]	0.13	NS[c]
Tumbarumba	Cold temperate forest	NS[c]	NS[c]	NS[c]	NS[c]	NS[c]	NS[c]	NS[c]	NS[c]	NS[c]	NS[c]	NS[c]	NS[c]

[a]Significant regression at $\alpha = 0.01$.
[b]Significant regression at $\alpha = 0.001$.
[c]NS is not significant.

At Tumbarumba, annual FI showed hourly patterns similar to those at Chaco Forest in summer (Figure 5). Significant differences (ANOVA, $F = 28.47$, $p < 0.01$, $n = 36$) were found among the FI values calculated over the four local times. Observations at the Australia open woodland savanna site, Howard Springs, showed increases of FI across the day (Figures 2b and 5). Observations at the sparse vegetated sites (Alice Springs and Sturt Plains) showed hourly variations in FI to be higher when EVI values were lower (EVI < 0.2), probably due to soil dynamics and vegetation effects, which corresponded with winter season (dry period, May–April) (Figure 5). FI values were very low throughout the available period and showed daily cycles with negative values. A consistent explanation of this behavior is the variation of temperature profile in dry sandy soils characteristic of this location [*Prigent et al*., 1999].

To better understand the relationship between soil temperature and FI at hourly scales, we evaluated the relation between FI and soil temperature at 8 cm depth (T_s) at Sturt Plains and Howard Springs (Alice Springs was not evaluated due to the lack of hourly T_s data during 2007–2009). At Howard Springs and Sturt Plains, there was a significant determination coefficient (R^2) (Table 5) between T_s and FI during dry winter period; however, both R^2 decrease during the rainy season.

Hourly trends of PI were related to different processes. At the Dry Chaco Forest and Tumbarumba sites, hourly variations and average values of PI were low across all seasons. In contrast, the other Australian sites showed strong hourly variations with a maximum at 1:30 h and 13:30 h (AMSR-E) and a minimum at 6:00 h and 18:00 h (WindSat). Similarly to FI, these variations can be related to hourly cycles of thermodynamic temperature at different depths inside the soil. We did not find a significant relation between PI and T_s at hourly temporal scale at Sturt Plains and Howard Springs (results not shown).

3.3. Summary of Diurnal and Seasonal Behavior of Passive Microwave Time Series

To summarize temporal microwave variations, we evaluated different regressions including all study areas (Figure 6 and Figure S1 in the supporting information). In dense vegetated areas (Dry Chaco Forest and Tumbarumba), PI is low, and FI depends on the canopy properties. The dynamics of FI is higher in Dry Chaco Forest, since it is partially deciduous and shows a moderate correlation between the two passive microwave indices ($r_{aa} = 0.62$; $r_{ad} = 0.53$, $p < 0.01$; $r_{wa} = 0.49$; $r_{wd} = 0.46$, $p < 0.05$, where r is the correlation coefficient, *aa* is the AMSR-E ascending, *ad* is the AMSR-E descending, *wa* is the WindSat ascending, and *wd* is the WindSat descending). The evergreen Tumbarumba forest has low correlation values at 6:00 h and 1.30 h ($r_{aa} = 0.45$; $r_{wd} = 0.27$, $p < 0.05$) due to the lack of well-defined seasonality. At the Howard Springs moderate biomass tropical woody savanna (62.4 t/ha), these two passive microwave indices were significantly correlated in this case ($r_{aa} = 0.82$; $r_{ad} = 0.71$; $r_{wa} = 0.84$; $r_{wd} = 0.82$, $p < 0.01$). In the less densely vegetated areas (Alice Springs and Sturt Plains), we calculated the correlation in two different situations: (i) one associated with low daily precipitation values (for Alice Springs days when the 8 day accumulated precipitation was lower than 50 mm/d and for Sturt Plains when the precipitation was lower than 100 mm/d) and (ii) with high precipitation values (opposite to (i)). At both sites, PI and FI were inversely correlated ($r_{aa} = -0.66$; $r_{ad} = -0.82$; $r_{wa} = -0.64$; $r_{wd} = -0.36$, $p < 0.01$) when soil temperatures were the dominant signal influence (85% of the data) but became directly correlated ($r_{aa} = 0.58$; $r_{ad} = 0.28$; $r_{wa} = 0.48$; $r_{wd} = 0.44$, $p < 0.05$) when soil moisture variations were the dominant influence (15% of the data showed this).

3.4. Eddy Covariance Flux Measurements of Evapotranspiration

The relationship between passive microwave observations and in situ eddy covariance flux measurements of latent energy (LE) showed a significant relation between LE with FI (Figure 7 and Figure S2 in the supporting

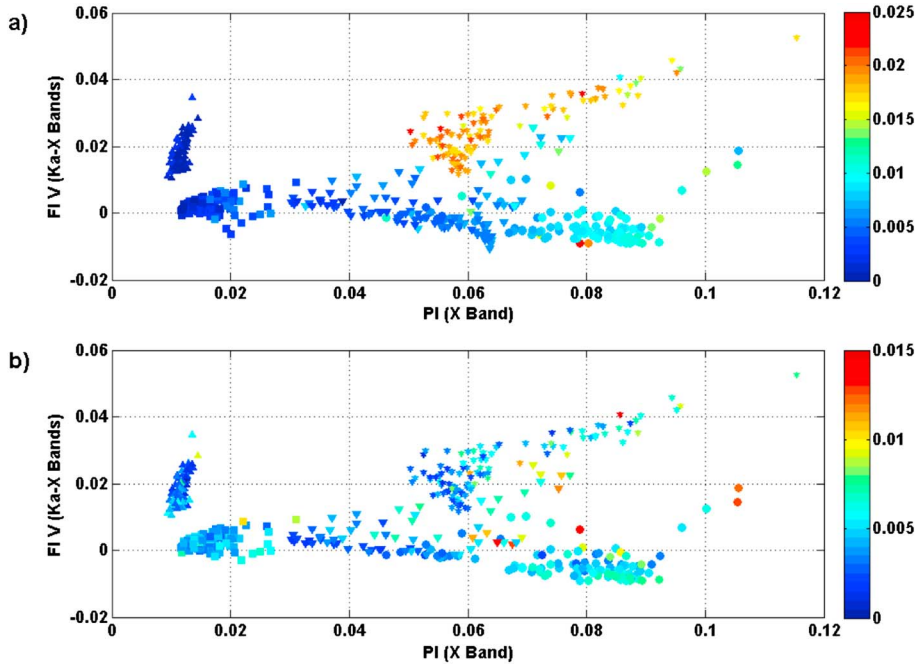

Figure 6. Mean multisensory 8 day FI versus PI scatterplot for 2007–2009. This figure shows the hourly component of both indices. (a) The color scale represents the standard deviation of daily PI values. (b) The color scale represents the standard deviation of daily FI values. The markers are upward pointing triangles for open forest (Dry Chaco Forest), asterisks for tropical open woodland savanna (Howard Springs), downward pointing triangles for semi arid savanna (Alice Springs), circles for grassland (Sturt Plains), and squares for wet temperate sclerophyll eucalypt forest (Tumbarumba).

information). Interestingly, the determination coefficient was positive and significant for Sturt Plains and Howard Springs sites and negative ($p < 0.01$) but nonsignificant for Tumbarumba ($p > 0.05$).

Finally, we found that PI (data not shown) was not significantly related to LE for Sturt Plains and Tumbarumba. There was a significant relation only at Howard Springs ($R^2_{aa} = 0.40$; $R^2_{ad} = 0.29$, $R^2_{wa} = 0.28$; $R^2_{wd} = 0.41$, $p < 0.01$).

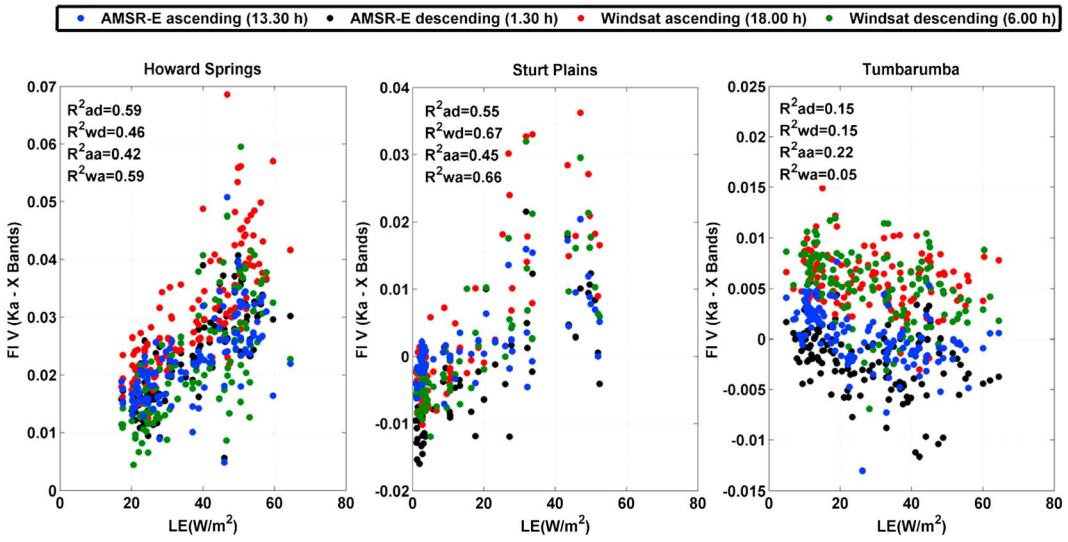

Figure 7. Scatterplot between 8 day FI and latent energy (LE) time series data for 2007–2009 for Howard Springs, Sturt Plain, and Tumbarumba, where R^2 is the determination coefficient specifically, R^2_d is the AMSR-E descensing, R^2_{wd} is the WindSat desending, R^2_{aa} is the AMSR-E ascending, and R^2_{wa} is the WindSat ascending.

4. Discussion

In this study we analyzed vegetation and soil contributions to the overall temporal behavior of two passive microwave indices in contrasting Southern Hemisphere ecosystems (tropical and semiarid savannas, temperature and xerophyte forest, and grassland).

To better interpret the microwave data, we used prior analyses made over Dry Chaco Forest [*Barraza et al*., 2014] as a benchmark case. Seasonal trends over this area were previously explained by *Barraza et al*. [2014] using a theoretical emission model accounting for changes in both LAI and vegetation moisture. MODIS LAI largely accounted for changes in FI seasonal trends (phenology), and short-term changes in FI were associated with vegetation moisture effects (e.g., hydric stress) [*Barraza et al*., 2014]. In this analysis, the observed inverse relation between MODIS EVI and FI was explained on the basis of the above-mentioned moisture-vegetation relationship. Moreover, this basic behavior was also found by *Li et al*. [2009] at Harvard Forest using different index definitions. This hypothesis is difficult to prove in the field, since direct measurements of canopy moisture are generally not available.

Results obtained for Dry Chaco Forest were not easily extendable to the Australian sites, where vegetation dynamics (EVI) showed more complex relations with the microwave indices. At Tumbarumba temperate site, covered by a dense evergreen sclerophyll forest, both microwave indices showed low seasonal variations, while the hourly variation of FI was similar to the one observed at Dry Chaco Forest during the summer.

For the other Australian sites, FI and PI dynamics controlled the interpretations of observed passive microwave index trends with vegetation biomass, soil moisture, and superficial soil emission. A significant relation was found between FI and PI with soil moisture in tropical open woody savannas (Howard Springs). Many contributing factors (e.g., soil moisture, superficial profile of soil temperature, and phenology) are required to explain the behavior of the two passive microwave indices in Alice Springs and Sturt Plains. In particular, in these sparse vegetated sites, the observed radiation was not simply produced at the air/soil interface, and FI variations can be explained by variations of temperature profile, in agreement with previous works [*Parinussa et al*., 2011; *Norouzi et al*., 2012].

As stated before, the estimation of evapotranspiration from satellite data for a general surface is a challenging inference problem. Although the physical basis of the problem was stated two decades ago, and the time series of passive microwave data can be interpreted in terms of changes of key biophysical variables (soil and vegetation moisture), the development of a general scheme for the estimation of ET from these data is still a complex problem. This is related to a key issue: the relations that are valid for one ecosystem (e.g., a decrease of vegetation moisture driving a reduction of ET and consequently increasing values of FI observed at dense forests) can be qualitatively different for another. Therefore, it is very important to understand the source of the observed emitted radiation before choosing a particular inference scheme. In this context, the FI versus PI scheme (Figure 6) presented in this study can be used to characterize ecosystems in terms of their PI and FI behavior.

In general, a significant relation does not imply causality. Nevertheless, our results also agree with the literature [*Prigent et al*., 1999; *Min and Lin*, 2006; *Li et al*., 2009; *Jones et al*., 2012; *Barraza et al*., 2014], showing that the FI versus PI relation provides a sound physical-biophysical scheme to characterize main hydrological dynamics of the ecosystem. Using this scheme, it can be seen that the methodologies developed by *Min and Lin* [2006] or *Barraza et al*. [2014] can only be applied for densely vegetated area, in which the key hypothesis required for the methodology is met. Moreover, although for these ecosystems the key processes which relate ET to microwave indices will be the same (decrease of vegetation moisture, decrease of ET, and increase of FI), the relation will be a function of the values of geometrical and dielectric characteristics of the canopy and, in general, will vary for different ecosystems.

From direct comparisons with in situ observations of latent energy (LE), FI was significantly related with LE for Howard Springs and Sturt Plains sites. At Tumbarumba, there was not much seasonality in FI or PI, which will effectively weaken the experimental relation between ET and microwave indices, similar to what occurs with MODIS vegetation index relations and ET. In spite of this, it is important to note that the relation between FI and LE at Tumbarumba is opposite to the one found for the other two sites. Interesting, *Yebra et al*. [2013] also shows negative correlations between normalized difference vegetation index and EVI and ET at this site. This suggests that microwave indices could only be used to estimate ET at regional scales using a land cover specific retrieval scheme. These results are in agreement with the ones obtained by *Min and Lin* [2006] and *Jones et al*. [2012].

5. Conclusion

Remote sensing indices are extremely useful tools in monitoring processes related to water and energy fluxes. In this study, we analyzed two passive microwave indices, FI and PI, over Southern Hemisphere ecosystems. Optical indices, environmental drivers, and eddy covariance measurements were also analyzed. We found different FI/PI behavior in differently types of ecosystems, which were related to the sensitivity of this indices to soil and vegetation characteristics. From Figure 6 and Figure S1 in the supporting information, it can be seen that

1. low values of PI and possible variations of FI can be associated with ecosystems, in which the overall emissivity is controlled by vegetation properties (LAI and vegetation moisture);
2. high values of PI and positive correlations between FI and PI variations are associated with ecosystems with moderate biomass and significant variations of soil moisture; and
3. high values of PI and negative correlations between FI and PI variations are associated with ecosystems, in which the overall emissivity is controlled by soil physical properties (thermodynamic temperature and possibly soil moisture vertical gradient).

We also found a significant relation between LE and FI across different ecosystems. This finding suggests the potential of passive microwave in monitoring vegetation/soil properties and the consequence of ecosystem exchange processes. Nevertheless, future work is required to develop and propose more robust methodologies for estimation of ET using diurnal and seasonal passive microwave observations.

Acknowledgments

This work was funded by MinCyT-CONAE-CONICET project 12. The authors specially wish to thank the reviewers, Roberto A. Fernandez and Javier Gyeng, for their valuable suggestions that significantly improved the paper. Part of this study was conducted through a visiting scholar appointment awarded to the author by the University of Technology, Sydney through funds from ARC-DP140102698 (Huete, CI). The author appreciates and acknowledges the OzFlux network and tower principal investigators for making the data freely available. Flux data provided here from Sturt Plains and Howard Springs were funded by the Australian Research Council (DP0772981 and DP130101566). Beringer is funded under an ARC FT (FT1110602). Support for collection and archiving was provided through the Australia Terrestrial Ecosystem Research Network (http://www.tern.org.au).

References

Asrar, G., M. Fuchs, E. T. Kanemasu, and J. L. Hatfield (1984), Estimating absorbed photosynthetic radiation and leaf area index from spectral reflectance in Wheat1, *Agron. J.*, *76*(2), 300–306, doi:10.2134/agronj1984.00021962007600020029x.

Barraza, V., F. Grings, P. Ferrazzoli, M. Salvia, M. Maas, R. Rahmoune, C. Vittucci, and H. Karszenbaum (2014), Monitoring vegetation moisture using passive microwave and optical indices in the Dry Chaco Forest, Argentina, *IEEE J. Sel. Top. Appl. Earth Obs. Remote Sens.*, *7*(2), 421–430, doi:10.1109/JSTARS.2013.2268011.

Beringer, J. (2013a), Sturt Plains OzFlux tower site OzFlux: Australian and New Zealand Flux Research and Monitoring, hdl:102.100.100/13772.

Beringer, J. (2013b), Howard Springs OzFlux tower site OzFlux: Australian and New Zealand Flux Research and Monitoring, hdl:102.100.100/13779.

Cleverly, J., N. Boulain, R. Villalobos-Vega, N. Grant, R. Faux, C. Wood, P. G. Cook, Q. Yu, A. Leigh, and D. Eamus (2013), Dynamics of component carbon fluxes in a semi-arid Acacia woodland, central Australia, *J. Geophys. Res. Biogeosci.*, *118*, 1168–1185, doi:10.1002/jgrg.20101.

Das, N. N., A. Colliander, S. K. Chan, E. G. Njoku, and L. Li (2014), Intercomparisons of brightness temperature observations over land from AMSR-E and WindSat, *IEEE Trans. Geosci. Remote Sens.*, *52*(1), 452–464, doi:10.1109/TGRS.2013.2241445.

Eamus, D., A. P. O'Grady, and L. Hutley (2000), Dry season conditions determine wet season water use in the wet-tropical savannas of northern Australia, *Tree Physiol.*, *20*(18), 1219–1226.

Eamus, D., J. Cleverly, N. Boulain, N. Grant, R. Faux, and R. Villalobos-Vega (2013), Carbon and water fluxes in an arid-zone Acacia savanna woodland: An analyses of seasonal patterns and responses to rainfall events, *Agric. For. Meteorolog.*, *182–183*, 225–238, doi:10.1016/j.agrformet.2013.04.020.

Engman, E. T., and N. Chauhan (1995), Status of microwave soil moisture measurements with remote sensing, *Remote Sens. Environ.*, *51*(1), 189–198, doi:10.1016/0034-4257(94)00074-W.

Ferrazzoli, P., L. Guerriero, S. Paloscia, P. Pampaloni, and D. Solimini (1992), Modeling polarization properties of emission from soil covered with vegetation, *IEEE Trans. Geosci. Remote Sens.*, *30*(1), 157–165.

Ferrazzoli, P., L. Guerriero, S. Paloscia, and P. Pampaloni (1995), Modeling X and Ka band emission from Leafy vegetation, *J. Electromagn. Waves Appl.*, *9*(3), 393–406, doi:10.1163/156939395X00541.

Gaiser, P. W., et al. (2004), The WindSat spaceborne polarimetric microwave radiometer: Sensor description and early orbit performance, *IEEE Trans. Geosci. Remote Sens.*, *42*(11), 2347–2361, doi:10.1109/TGRS.2004.836867.

Gasparri, N. I., and G. Baldi (2013), Regional patterns and controls of biomass in semiarid woodlands: Lessons from the Northern Argentina Dry Chaco, *Reg. Environ. Change*, *1–14*, doi:10.1007/s10113-013-0422-x.

González, M. H., and O. K. Flores (2010), Análisis de la precipitación en la llanura chaqueña argentina y su relación con el comportamiento de la circulación atmosférica y las temperaturas de la superficie del mar, *Meteorologica*, *35*(2), 53–66.

Granger, R. (2000), Satellite-derived estimates of evapotranspiration in the Gediz basin, *J. Hydrol.*, *229*(1–2), 70–76, doi:10.1016/S0022-1694(99)00200-0.

Hansen, M. C., and B. Reed (2000), A comparison of the IGBP DISCover and University of Maryland 1 km global land cover products, *Int. J. Remote Sens.*, *21*(6–7), 1365–1373, doi:10.1080/014311600210218.

Huete, A., K. Didan, T. Miura, E. P. Rodriguez, X. Gao, and L. G. Ferreira (2002), Overview of the radiometric and biophysical performance of the MODIS vegetation indices, *Remote Sens. Environ.*, *83*(1–2), 195–213, doi:10.1016/S0034-4257(02)00096-2.

Hutley, L. B., J. Beringer, P. R. Isaac, J. M. Hacker, and L. A. Cernusak (2011), A sub-continental scale living laboratory: Spatial patterns of savanna vegetation over a rainfall gradient in northern Australia, *Agric. For. Meteorol.*, *151*(11), 1417–1428, doi:10.1016/j.agrformet.2011.03.002.

Jackson, T. J. (1997), Soil moisture estimation using special satellite microwave/imager satellite data over a grassland region, *Water Resour. Res.*, *33*(6), 1475–1484, doi:10.1029/97WR00661.

Jones, M. O., J. S. Kimball, L. A. Jones, and K. C. McDonald (2012), Satellite passive microwave detection of North America start of season, *Remote Sens. Environ.*, *123*, 324–333, doi:10.1016/j.rse.2012.03.025.

Kanniah, K. D., J. Beringer, and L. B. Hutley (2011), Environmental controls on the spatial variability of savanna productivity in the Northern Territory, Australia, *Agric. For. Meteorol.*, *151*, 1429–1439, doi:10.1016/j.agrformet.2011.06.009.

Kawanishi, T., T. Sezai, Y. Ito, K. Imaoka, T. Takeshima, Y. Ishido, A. Shibata, M. Miura, H. Inahata, and R. W. Spencer (2003), The Advanced Microwave Scanning Radiometer for the Earth Observing System (AMSR-E), NASDA's contribution to the EOS for global energy and water cycle studies, *IEEE Trans. Geosci. Remote Sens.*, *41*(2), 184–194, doi:10.1109/TGRS.2002.808331.

Leuning, R., H. A. Cleugh, S. J. Zegelin, and D. Hughes (2005), Carbon and water fluxes over a temperate Eucalyptus forest and a tropical wet/dry savanna in Australia: Measurements and comparison with MODIS remote sensing estimates, *Agric. For. Meteorol.*, *129*(3–4), 151–173, doi:10.1016/j.agrformet.2004.12.004.

Li, R., Q. Min, and B. Lin (2009), Estimation of evapotranspiration in a mid-latitude forest using the Microwave Emissivity Difference Vegetation Index (EDVI), *Remote Sens. Environ.*, *113*(9), 2011–2018, doi:10.1016/j.rse.2009.05.007.

Ma, X., et al. (2013), Spatial patterns and temporal dynamics in savanna vegetation phenology across the North Australian Tropical Transect, *Remote Sens. Environ.*, *139*, 97–115, doi:10.1016/j.rse.2013.07.030.

Min, Q., and B. Lin (2006), Remote sensing of evapotranspiration and carbon uptake at Harvard Forest, *Remote Sens. Environ.*, *100*(3), 379–387, doi:10.1016/j.rse.2005.10.020.

Morello, J. (1974), *Las grandes unidades de vegetación y ambiente del Chaco argentino: pt. Vegetación y ambiente de la provincia del Chaco*, Secretaria de Estado de Agricultura y Ganadería de la Nación, Instituto Nacional de Tecnología Agropecuaria, Centro de Investigaciones de Recursos Naturales, Buenos Aires.

Myneni, R. B., F. G. Hall, P. J. Sellers, and A. L. Marshak (1995), The interpretation of spectral vegetation indexes, *IEEE Trans. Geosci. Remote Sens.*, *33*(2), 481–486, doi:10.1109/36.377948.

Myneni, R. B., R. Ramakrishna, R. Nemani, and S. W. Running (1997), Estimation of global leaf area index and absorbed par using radiative transfer models, *IEEE Trans. Geosci. Remote Sens.*, *35*(6), 1380–1393, doi:10.1109/36.649788.

Norouzi, H., W. Rossow, M. Temimi, C. Prigent, M. Azarderakhsh, S. Boukabara, and R. Khanbilvardi (2012), Using microwave brightness temperature diurnal cycle to improve emissivity retrievals over land, *Remote Sens. Environ.*, *123*, 470–482, doi:10.1016/j.rse.2012.04.015.

Paloscia, S., and P. Pampaloni (1988), Microwave polarization index for monitoring vegetation growth, *IEEE Trans. Geosci. Remote Sens.*, *26*(5), 617–621, doi:10.1109/36.7687.

Paloscia, S., and P. Pampaloni (1992), Microwave vegetation indexes for detecting biomass and water conditions of agricultural crops, *Remote Sens. Environ.*, *40*(1), 15–26, doi:10.1016/0034-4257(92)90123-2.

Parinussa, R. M., T. R. H. Holmes, M. T. Yilmaz, and W. T. Crow (2011), The impact of land surface temperature on soil moisture anomaly detection from passive microwave observations, *Hydrol. Earth Syst. Sci.*, *15*(10), 3135–3151, doi:10.5194/hess-15-3135-2011.

Prigent, C., W. B. Rossow, E. Matthews, and B. Marticorena (1999), Microwave radiometric signatures of different surface types in deserts, *J. Geophys. Res.*, *104*(D10), 12,147–12,158, doi:10.1029/1999JD900153.

Richardson, A. D., and D. Y. Hollinger (2005), Statistical modeling of ecosystem respiration using eddy covariance data: Maximum likelihood parameter estimation, and Monte Carlo simulation of model and parameter uncertainty, applied to three simple models, *Agric. For. Meteorol.*, *131*(3–4), 191–208, doi:10.1016/j.agrformet.2005.05.008.

Sea, W. B., P. Choler, J. Beringer, R. A. Weinmann, L. B. Hutley, and R. Leuning (2011), Documenting improvement in leaf area index estimates from MODIS using hemispherical photos for Australian savannas, *Agric. For. Meteorol.*, *151*(11), 1453–1461, doi:10.1016/j.agrformet.2010.12.006.

Strahler, A. H., et al. (2008), Retrieval of forest structural parameters using a ground-based lidar instrument (Echidna), *Can. J. Remote Sens.*, *34*(S2), S426–S440, doi:10.5589/m08-046.

Taylor, J. A., and D. Tulloch (1985), Rainfall in the wet-dry tropics: Extreme events at Darwin and similarities between years during the period 1870–1983 inclusive, *Aus. J. Ecol.*, *10*(3), 281–295, doi:10.1111/j.1442-9993.1985.tb00890.x.

van Gorsel, E. (2013), Tumbarumba OzFlux tower site OzFlux: Australian and New Zealand Flux Research and Monitoring, hdl:102.100.100/13791sTURT.

van Gorsel, E., et al. (2013), Primary and secondary effects of climate variability on net ecosystem carbon exchange in an evergreen Eucalyptus forest, *Agric. For. Meteorol.*, doi:10.1016/j.agrformet.2013.04.027.

Vermote, E. F., and A. Vermeulen (1999), MODIS Algorithm Technical Background Document, Atmospheric Correction Algorithm: Spectral Reflectances (MOD09), Version 4.0, April 1999. [Available at http://modis.gsfc.nasa.gov/data/atbd/atbd_mod08.pdf.]

Yebra, M., A. Van Dijk, R. Leuning, A. Huete, and J. P. Guerschman (2013), Evaluation of optical remote sensing to estimate actual evapotranspiration and canopy conductance, *Remote Sens. Environ.*, *129*, 250–261, doi:10.1016/j.rse.2012.11.004.